International Journal of Geographical Information Science

Automated generation of concentric circles metro maps using mixed-integer optimization

Yingying Xu[1], Ho-Yin Chan[2], and Anthony Chen[1,3*]

[1] Department of Civil and Environmental Engineering, The Hong Kong Polytechnic University, Kowloon, Hong Kong
[2] Transport Studies Unit, School of Geography and the Environment, University of Oxford, UK
[3] Hong Kong Branch of National Rail Transit Electrification and Automation Engineering Technology, The Hong Kong Polytechnic University, Kowloon, Hong Kong

* Corresponding author: anthony.chen@polyu.edu.hk

Abstract

Concentric circles (CC) map design is an alternative schematic representation for metro systems. Compared to the traditional octo-linear maps, CC maps simply the perception of the network by putting visual accent on circular line patterns. This design offers new insights into schematic drawings for metro systems. At present, automated mapping literature focuses mainly on the traditional octo-linear design using the optimization approach. Design criteria are modeled as constraints and/or objective functions in a constrained mixed-integer optimization program. Nevertheless, there are only a few studies focus on the automated CC map drawing. In this article, we develop an automatic CC map drawing method by adopting map design criteria as a mixed-integer programming (MIP) problem. Numerical experiments are conducted with (a) a simple network that illustrates the modeling procedure in detail, and (b) two real-world metro networks in Vienna and Montréal to analyze the effects of the choice of map center and parameter settings.

Keywords: Schematic map; Concentric circles map; Metro network; Automatic map drawing; Mixed-integer programming

Highlights

- We implement an optimization map-drawing procedure in drawing concentric circles metro maps
- We model the usability of maps into two major design criteria, namely topographcity and simplicity
- Our proposed algorithm allows generating prototypes quickly with flexibility
- We apply the proposed model in small, medium, large real-world metro networks

Final version

Xu, Y., Chan, H. Y., & Chen, A. (2022). Automated generation of concentric circles metro maps using mixed-integer optimization. *International Journal of Geographical Information Science*, 1-26.

1. Introduction

Humanity has faced the challenge of network visualization way before the advent of the computer. Although the first underground railway opened in 1863 (Wolmar, 2009), the first schematic metro map, resembling modern metro maps was created only in 1933 by Harry Beck (Roberts, 2014). He realized that the usability of a network visualization is based on the simplification of a real system, which is more important than the geographical accuracy. This is known as octolinearity, which is commonly believed as a golden design rule used worldwide to depict railway networks in official maps (Ovenden, 2015). In 1989, Erik Spiekermann proposed a novel radical design with multiple concentric circles for the reunified Berlin U-Bahn/S-Bahn network (Roberts, 2013). The concept of concentric circles (CC) has not yet been investigated until recently Roberts (2013) promotes the idea by emphasizing its high structural coherence, other than the simplification in octo-linearity entailed in removing complex line trajectories. He suggested that CC maps promote better network learning and memorizing than the octo-linear one by reducing the cognitive load. Although recent usability studies indicated that the high coherence of its overall structure is adequate to compensate for the poor simplicity of its line trajectories (Roberts, 2019; Roberts et al., 2016), they could not deny the high attractiveness of this drawing style, which generated interests and responses on the internet (Chan, 2018; Konovalov, 2016; Tseng, 2017), by giving users a choice of metro map design.

In recent years, one can observe an increasing number of studies in automated network visualization. For the octo-linear map design, a force-directed graph layout algorithm (Hong et al., 2006; Stott et al., 2011) and optimization algorithm (Lan et al., 2019; Nöllenburg and Wolff, 2011; Sester, 2005; Wang and Chi, 2011; Wang and Peng, 2016) are widely used to guarantee the octo-linearity of the line segments. Different from the traditional octo-linear design with straight lines (vertically or horizontally) and 45° angles, circular and radial segments are fundamental elements in the concentric circles design where lines go around or traverse the center. However, there are only a few studies focus on the concentric circles map automatic drawing (Barth, 2016; Fink et al., 2014). In this article, we develop a mixed-integer programming (MIP) model to automatically draw the concentric circles map by integrating the design criteria from the aesthetics perspective (Roberts, 2014). We demonstrate the feasibility and effectiveness of the method using a simple network and two real-word metro networks: the Vienna metro network and the Montréal metro network.

2. Related works

A common technique used to pursue simplicity in the design of complex network maps is to create a schematized representation. When comparing schematic maps worldwide, the dominance of octolinearity (i.e., drawn with only horizontal, vertical, and 45° diagonal straight lines) is clear (Ovenden, 2015). Recent research in automated octilinear schematic map design usually based on iterative procedure (Bertault, 2000; Frick et al., 1995; Hong et al., 2006; Kozo Sugiyama; Kazuo Misue, 1995; Li and Dong, 2010; Stott et al., 2011) and optimization model (Lan et al., 2019; Nöllenburg and Wolff, 2011). Hong et al. (2006) generate the scheme map using five methods based on three force-directed approaches: graph embedder (GEM) (Frick et al., 1995), force-directed algorithm (PrEd) (Bertault, 2000), and a magnetic spring algorithm (Kozo Sugiyama; Kazuo Misue, 1995). For each iteration, the position of the vertices is updated to identify a good metro map graph based on the qualitative criteria. Stott et al. (2011) adopt a Hill-Climbing algorithm by moving the stations and labels iteratively based on station criteria and label criteria, which are calculated to judge the quality of the map. Li and Dong (2010)

propose a stroke-based method, where line segments are formed as strokes, to generate the schematic map. To improve readability of the schematic maps, congested area is often enlarged, which can be incorporated in the stroke-based method (Ti and Li, 2014). The optimization model is another way to identify the position of stations in schematic maps. Nöllenburg and Wolff (2011) used mix-integer linear programming (MIP) to model the octo-inearity as a hard constraint to find a optimal metro map that minimizes the use of bends and lengths as well as distortion. Binary variables are introduced for analyzing the design rules, which are formulated by constraints in the optimization model. General principles are also integrated into the MIP to improve the clarity and aesthetics of generated schematic maps (Lan et al., 2019).

In octilinear scheme map design, many design criteria are used to guarantee the octolinearity and aesthetics in both iterative approach and optimization method. Li (2015) formulate four principles for schematization: preservation of the topological relationship, preservation of the main structure, relative in position, and relative in length. These principles are illustrated to specified constraints that are used in MIP (Lan et al., 2019). The first two principles should never be violated, which are important for the map readability. The last two principles constrain the station and link characteristics to improve the aesthetics of the scheme map. Nöllenburg and Wolff (2011) gives a substantial set, for example, keep line trajectories as straight as possible, space stations evenly, station labels should not occlude lines, and relative positions of stations should be preserved. The research method and design criteria for automatically octilinear scheme map drawing is summarized in **Table 1**.

Roberts et al. (2013) argued that there is no scientific support in the psychological literature for the octolinearity as a gold standard belief in view of map usability. Following this, few attempts have been made to explore whether alternatives might result in better designs. Roberts (2013) show that the curvilinear design, which comprises only Bézier curves improved objective usability in terms of shorter journey planning times. The curvilinear schematic map simplifies the line trajectories and avoid visually disruptive bends that are more friendly for users to trace the metro lines (Fink et al., 2012). To automatic generate the curvilinear schematic map, Fink et al. (2012) use a force-directed algorithm which minimizing the usage of curves in one line. In addition to smoothing the harsh corners with curves, Roberts et al. (2016), suggested the concentric circles version, whose lines are drawn as circles with a common center, improved subjective usability in encouraging map engagement and more frequent use of public transport facilities. These refute the gold standard conjecture of the octilinear design, and it would be reasonable to suggest that we cannot overlook other possible alternatives.

To generate the concentric circle map algorithmically, Fink et al. (2014) adopt the mixed-integer programming to generate the concentric circle scheme map for Vienna and Montréal metro networks. However, the approach is not applicable in larger networks and further constraint simplification is needed. Barth (2016) develop another algorithm which have been applied in Montréal and London to draw the concentric circle map automatically. However, these approach offers very little flexibility to the designers who are pursuing a balance rather than optimal solution from the aesthetics perspective. In this article, we focus on the concentric circle design which stands as one of the most indelible designs in recent literature (Chan et al., 2021; Roberts, 2019, 2013; Saidi et al., 2017, 2016a, 2016b; Szabo and Genge, 2019; Wu et al., 2020). We compiled the criteria for effective map design proposed by Roberts (2014), which consists of five criteria namely simplicity, coherence, harmony, balance, and topographicity, in order to maximize the map usability and engagement. In our approach, the criteria are described more detailed to modelled in the objective of the optimization program.

Table 1. Summary of automated schematic map drawing approaches

Design rules	Research method		Design criteria	Example
Octilinear	Iterative procedure	Force-directed algorithm	Line straightness, no edge crossing, no overlapping of labels, octilinear direction, line distinctly	(Bertault, 2000; Frick et al., 1995; Hong et al., 2006; Kozo Sugiyama; Kazuo Misue, 1995)
		Stroke-based method	Network simplicity and clarity	(Li and Dong, 2010; Ti and Li, 2014)
		Hill climbing	Angular resolution, edge length, balanced edge length, line straightness, octolinearity, label setting	(Stott et al., 2011)
	Optimization model	Mix-integer programming	Octolinearity, preserve the network topology, avoid bends, preserve the relative position between stations, uniform edge length, label should not obscure each other, distinctive line color	(Lan et al., 2019; Nöllenburg and Wolff, 2011)
Curvilinear	Force-directed algorithm		Minimize total Bezier curves for lines to avoid inflection.	(Fink et al., 2012)
Concentric circles	Min-cost-flow		Minimize total bends	(Barth, 2016)
	Mixed-integer program		Minimize total bends, stations should be placed closer to geographic locations	(Fink et al., 2014)

3. Methodology

In this article, we model the concentric circles map drawing as MIP where the design criteria are modelled as the optimization objective. We illustrate this model in detail in the following section.

3.1 Network representation

The geographic information of stations and the central point are input data which need to be transformed to Cartesian coordinates. And then, we convert the coordinate of stations to polar coordinate which is easy to describe the ring and radial line section. The data preparation process is described in **Fig. 1**.

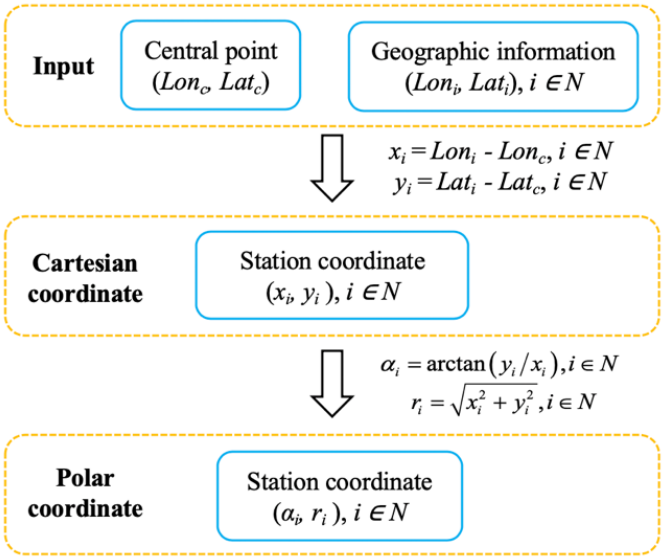

Fig. 1. Data preparation

In concentric circles maps, stations are connected by either ring or radial line segments. To simplify the expression of the stations and links, we use polar coordinates to represent the position. In concentric circles map drawing, there are two basic elements of drawing: vertices and link section. Vertices are described by the angle from the reference direction and the distance from the pole. Link section between adjacent stations can be represent by the angle of the radial line segment in the link section as shown in **Fig. 2**.

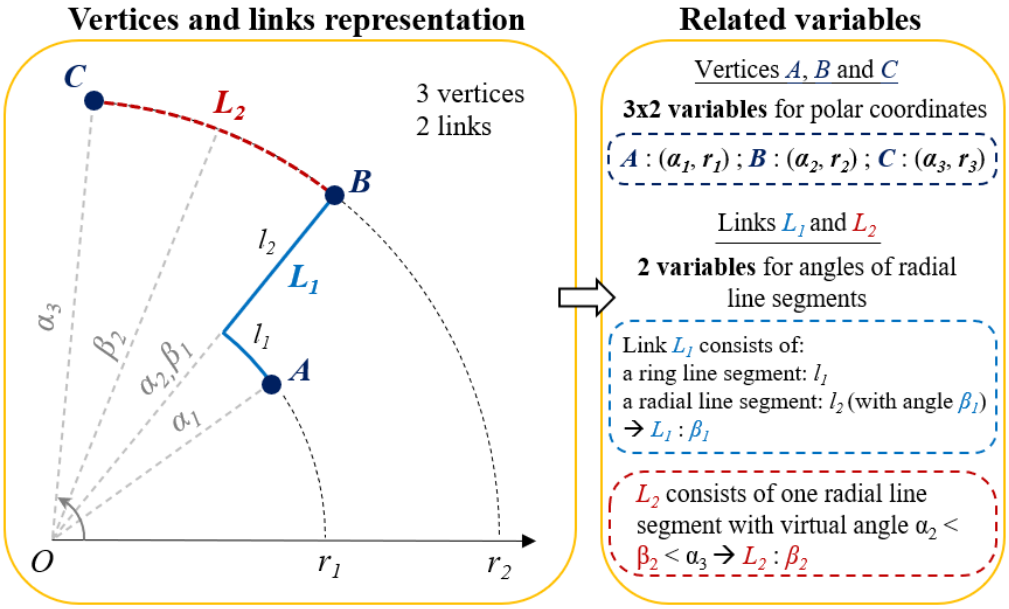

Fig. 2. Example of network representation

For instance, as shown in **Fig. 2**, there are three vertices *A*, *B*, and *C*, and two link sections L_1 and L_2 connected these vertices. For each vertex, two variables, (α_i, r_i) for $i \in N$, are needed to describe the location of the point. Given the information of vertices, links connected the adjacent stations can be represent by one variable, β_p for $p \in L$, which shows the angle of the radial line segment in this link. For example, link L_1, connected vertices *A* and *B*, can be divide by a ring line segment l_1 and a radial line segment l_2. l_2 with angle β_1 can be described by [β_1,

$r_1 < r < r_2$]. r_1 and r_2 are the radii of vertices *A* and *B* respectively. For l_1, the radii are fixed with the angle in a range: [r_1, $\alpha_1 < \beta < \beta_1$]. Thus, the link section is determined given the angle of radial line segment l_2. For the link section without radial line segment (e.g., L_2), we can give a virtual radial line segment with angle β_2 ($\alpha_2 < \beta_2 < \alpha_3$). Since the radii of the virtual line is the same, it does not affect the map display.

3.2 Binary variables

We adopt two types of binary variables from Fink et al. (2014) as intermediate variables to facilitate the calculation of the number of bends. Type *X* variable is related to the relations between angles of vertices α_i and link segments β_p. Either of the three relations exists: (1) $\alpha_i < \beta_p$; (2) $\alpha_i = \beta_p$; (3) $\alpha_i > \beta_p$. Thus, angle relation $AR = \{\alpha_i < \beta_p, \alpha_i = \beta_p, \alpha_i > \beta_p\}$. X_{AR} equals to 1 if angle relation *AR* is satisfied. Type *Y* variable is related the relations of between two radius of vertices r_i, r_j. Similarly, either of the three relations exists: (1) $r_i < r_j$; (2) $r_i = r_j$; (3) $r_i > r_j$. Thus, radius relation $RR = \{ r_i < r_j, r_i = r_j, r_i > r_j \}$. Y_{RR} equals to 1 if radius relation *RR* is satisfied. Eqs. (1-6) are constraints used to ensure the binary variables have value 1 when corresponding relations are satisfied. In Eq. (1), $\alpha_i < \beta_p$ has to hold when $X_{\alpha i < \beta p} = 1$. Similar formulation is adopted for binary variables $Y_{ri < rj}$ in Eq. (4). In Eqs. (2-3), when $X_{\alpha i = \beta p} = 1$, $\alpha_i \le \beta_p$ and $\beta_p \le \alpha_i$ have to hold, which equivalent to $\alpha_i = \beta_p$. Again, Similar formulations are adopted for Eqs. (5)-(6). Those constraints mathematically descripted as:

$$\alpha_i + \varepsilon < \beta_p + 2\pi\left(1 - X_{\alpha_i < \beta_p}\right) \quad (1)$$

$$\alpha_i \le \beta_p + 2\pi\left(1 - X_{\alpha_i = \beta_p}\right) \quad (2)$$

$$\beta_p \le \alpha_i + 2\pi\left(1 - X_{\alpha_i = \beta_p}\right) \quad (3)$$

$$r_i + \varepsilon < r_j + M\left(1 - Y_{r_i < r_j}\right) \quad (4)$$

$$r_i \le r_j + M\left(1 - Y_{r_i = r_j}\right) \quad (5)$$

$$r_j \le r_i + M\left(1 - Y_{r_i = r_j}\right) \quad (6)$$

where $\mathcal{E}$ is a small value of angle and *M* is a large number.

Eqs. (7)-(8) are constraints used to make sure that only one binary variable in each type take the value of 1, mathematically as:

$$X_{\alpha_i < \beta_p} + X_{\beta_p < \alpha_i} + X_{\alpha_i = \beta_p} = 1 \quad (7)$$

$$Y_{r_i < r_j} + Y_{r_i < r_j} + Y_{r_i = r_j} = 1 \quad (8)$$

Take the simple network (three vertices and two links) shown in **Fig. 2** as an example. For edge *A*-*B*, we have to determine the angle relations of vertex *A* with α_1 and link L_1 with β_1. For $\alpha_1 < \beta_1$, $X_{\alpha 1 < \beta 1} = 1$. According to Eq. (1), when $X_{\alpha 1 < \beta 1} = 1$, $\alpha_1 + \mathcal{E} < \beta_1$ gives $\alpha_1 < \beta_1$. Thus, $\alpha_1 < \beta_1$ holds. For edge *B*-*C*, we have to determine the relations of vertices *B* and *C* with α_1 and α_2 respectively. For $r_2 = r_3$, $X_{r2=r3} = 1$. According to Eqs (5-6), when $X_{r2=r3} = 1$, $r_2 \le r_3$ and $r_3 \le r_2$ give $r_2 = r_3$. Thus, $r_2 = r_3$ holds. **Table 2** summarized the value of binary variables with the example network.

Table 2. Value of binary variables of the example network

Edge	Relations		Type *X*			Type *Y*		
	Vertex	Link	$\alpha_i < \beta_p$	$\alpha_i = \beta_p$	$\alpha_i > \beta_p$	$r_i < r_j$	$r_i = r_j$	$r_i > r_j$
A-B	*A*	L_1	1	0	0	1	0	0
	B	L_1	0	1	0			
B-C	*B*	L_2	1	0	0	0	1	0
	C	L_2	0	0	1			

3.3 Map efficiency criteria

We adopt the framework of efficient map design by Roberts (2014, 2013), who promotes the concentric circles style of drawing. The framework consists of two separate aspects, map usability and engagement, to evaluating a map. Map usability and engagement concern objective and subjective measurements respectively. We focus on the measurable objective aspect, which includes simplicity, coherence, balance, and topographicity. Simplicity emphasizes the individual line trajectories bend as few as possible while topographicity restricts the turning point of lines at stations to avoid excessive distortion. Balance focus on the station level in terms of density gradients. Coherence concerns overall map level, requiring higher-order measures of relatedness between lines, which is harder to quantify. We assume that lines in concentric circles maps are optimized in coherence considering all lines have the same common center, as discussed in Roberts et al. (2016). Therefore, the remaining questions for optimizing line trajectories are how to achieve simplicity with less bends while minimizing topographical distortion. In our MIP model, we formulate the (a) **topographicity** and (b) **simplicity** in the optimization objectives and constraints. Balance is not going to be discussed in this article as it is likely to be a second steps to placing the intermediate stations after generating the line trajectories with interchange and terminal stations.

3.3.1 Topographicity

Topographicity requires the station in the scheme map should be placed as close to their original location as possible. We preserve the relative location of the stations which is one of the general principles for scheme network map (Li, 2015), and minimize the location distortion from original layout which make it easy for users to identify the stations on the map.

3.3.1.1 Preserving the relative position

The relative position of each station should be preserved to facilitate the usability of schematic map. The relativity in position can be modeled by the relative direction, such as north, northwest, west, or the relative quadrant type described in cartesian coordinates (Lan et al., 2019) as shown in **Fig. 3**. The relative position of node *A* and *B* can be expressed by: *B* is in the northeast of *A* in geographical representation, or *B* is in the quadrant 1 of *A* using cartesian coordinates. The relative position is preserved if the relative direction or the relative quadrant do not change in the schematic map.

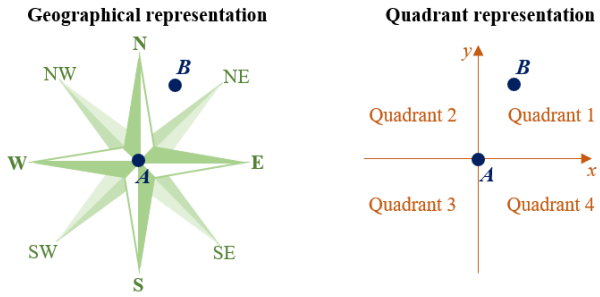

Fig. 3. Relative position of two vertices

In concentric circle maps, we preserve the relativity in position by keeping the relationship of the angle and radii unchanged which can be modelled mathematically

$$\alpha_i \le \alpha_j \text{ if } \alpha_i^o \le \alpha_j^o, i, j \in N \quad (9)$$

$$\alpha_i \ge \alpha_j \text{ if } \alpha_i^o \ge \alpha_j^o, i, j \in N \quad (10)$$

$$r_i \le r_j \text{ if } r_i^o \le r_j^o, i, j \in N \quad (11)$$

$$r_i \ge r_j \text{ if } r_i^o \ge r_j^o, i, j \in N \quad (12)$$

where $(\alpha_i^o, r_i^o), (\alpha_j^o, r_j^o)$ are the geographic position of station *i* and *j*.

In **Fig. 4**, B (α_2, r_2) is the position of vertex B^o in the schematic map. As $\alpha_1{}^o < \alpha_2{}^o$ and $r_1{}^o < r_2{}^o$, the location for vertex A in the schematic map follows $\alpha_1 < \alpha_2$ and $r_1 < r_2$ (the shadow area) that ensure the relative position of stations are reserved.

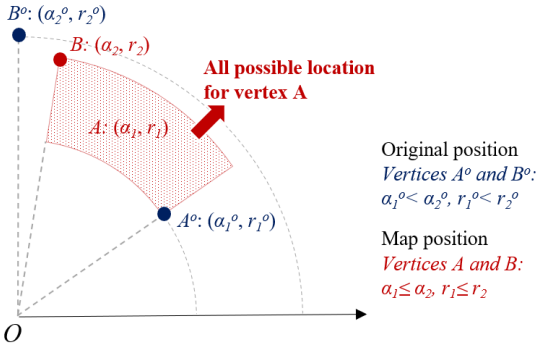

Fig. 4. Example of relative position in concentric circle map

3.3.1.2 Location distortion

Location distortion is adopted to characterize the gap between the mapped location and their geographic one. Location distortion is quantified by the sum of absolute difference of angles and radius individually. Two spatial properties, angular (direction) distortion *AD* and distance (linear) distortion *DD* is addressed, mathematically descripted as:

$$AD_i = \alpha_i - \alpha_i^o, i \in N \quad (13)$$

$$DD_i = r_i - r_i^o, i \in N \quad (14)$$

Thus, for an optimal solution, the stations are placed close to their geographic location can be realized by minimizing the absolute value of distortion for all stations as:

$$Min \sum_{i \in N} |AD_i| + \sum_{i \in N} |DD_i| \quad (15)$$

3.3.2 Simplicity

Simplicity requires lines should have as less bends as possible. In concentric circles maps, there are two types of bends: bends for edges *BE* and bends for traversing stations *BT*. As shown in **Fig. 5**, there are two bends for edge between station *A* and *B*. Bends for traversing stations happened on the vertices which have ring line segment and radial line segment on both side of the point. We aim at minimizing the number of bends for both types in the generated map to achieve simplicity.

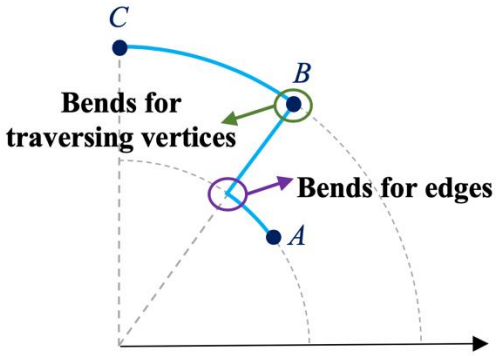

Fig. 5. Example of bends in concentric circles map

Thus, for an optimal solution, lines are as simple as possible by minimizing all type of bends for all lines as:

$$Min\sum_{p\in L} BE_p + \sum_{i\in N} BV_i \tag{16}$$

The number of bends can be calculated using the binary variables described in the next sub-sections.

3.3.2.1 Bends for the edges

In concentric circles map drawings, the line trajectories only include radial line segment and ring line segment. The edge between two adjacent stations has bends if there have both ring line segment and ring line segment between the vertices. For two stations *A* (α_1, r_1) and *B* (α_2, r_2), there has no bend if $\alpha_1 = \alpha_2$ or $r_1 = r_2$. If the angle β_1 of the radial line segment between the stations equal to the angle of one of the stations, which means $\alpha_1 = \beta_1$ or $\beta_1 = \alpha_2$, there is only one bend between the station. There are at most two bends for the edge under $\alpha_1 \neq \beta_1$ and $\beta_1 \neq \alpha_2$. The four possible line trajectories between two adjacent stations are given in **Fig. 6**.

- *No bend*. As shown in Fig. 6(a) and (b), there have no bend between station *A* and *B*. In (a), the radii of the vertices are the same, which means $Y_{r1=r2} = 1$. The ring line segment is described with a virtual angle β_1 where $\alpha_2 < \beta_1 < \alpha_1$, and $X_{\alpha1=\beta1} = X_{\alpha2=\beta1} = 0$. In (b), the radial line segment is described with angle β_1, where $\beta_1 = \alpha_1 = \alpha_2$, and thus $X_{\alpha1=\beta1} = X_{\alpha2=\beta1} = 1$.
- *One bend.* As shown in Fig. 6(c), there is one bend between station *A* and *B*. The angle of link section equals to the angle of one vertex. In this case, $X_{\alpha1=\beta1} = X_{\alpha2=\beta1} = 0$ and $Y_{r1=r2} = 0$.
- *Two bends.* For the edge with two bends, the angle of the stations and radial link segment satisfied $\alpha_1 \neq \beta_1$, $\beta_1 \neq \alpha_2$ and $r_1 \neq r_2$. In this case, $X_{\alpha1=\beta1} = X_{\alpha2=\beta1} = 0$ and $Y_{r1=r2} = 0$.

By analyzing all possible line trajectories between adjacent stations, we can formulate the number of bends for each edge *p* as

$$BE_p = \left(1 - X_{\alpha_i = \beta_p}\right) + \left(1 - X_{\alpha_j = \beta_p}\right) - 2 \times Y_{r_i = r_j}, p \in L \tag{17}$$

where *i* and *j* are vertices connecters link *p*.

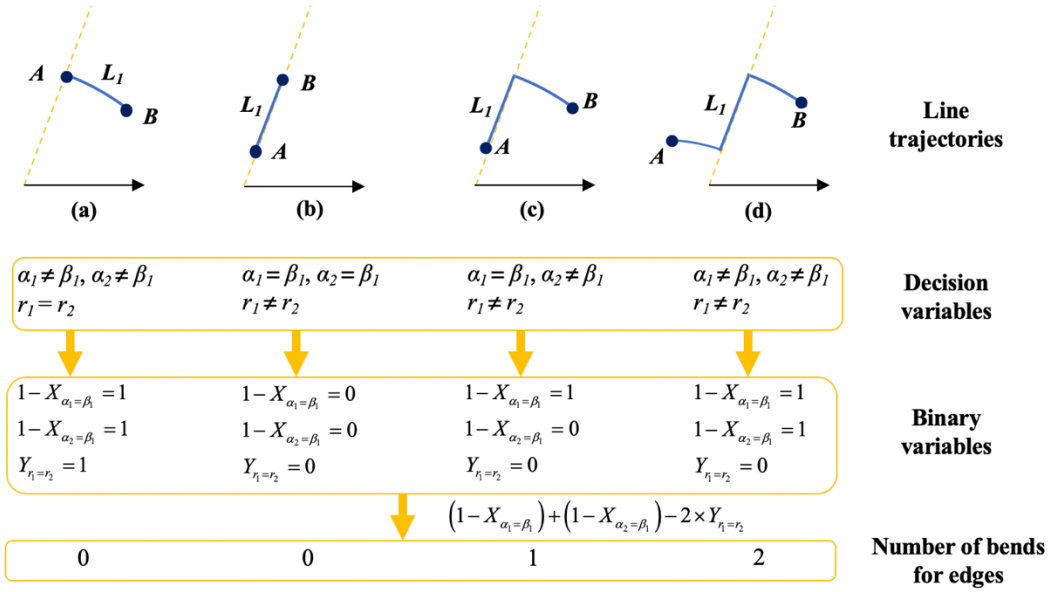

Fig. 6. Four possible line trajectories between two adjacent stations

3.3.2.2 Bends for traversing vertices

Similar to the bends between adjacent vertices, we can formulate the numbers of bends for line traversing vertices by analyzing all possible line trajectories traversing stations. As shown in Fig. 7, there exist bend traversing station *B* when the line segments on both sides are ring line and radial line respectively. For radial line segment as shown in **Fig. 7 (a)**, $\alpha_2 = \beta_1$, and for the ring line segment, $\alpha_2 \neq \beta_2$. If there is no bends traversing stations, the angle of the station equals or not equal to the angle of both side link section at once as shown in **Fig. 7 (b)** and **(c)**.

We can formulate the number of bends that the lines make traversing station *i* by

$$BV_i = \left| X_{\alpha_i = \beta_p} - X_{\alpha_j = \beta_q} \right|, i \in N \tag{18}$$

where β_p and β_q are the angles of link section connected station *i*.

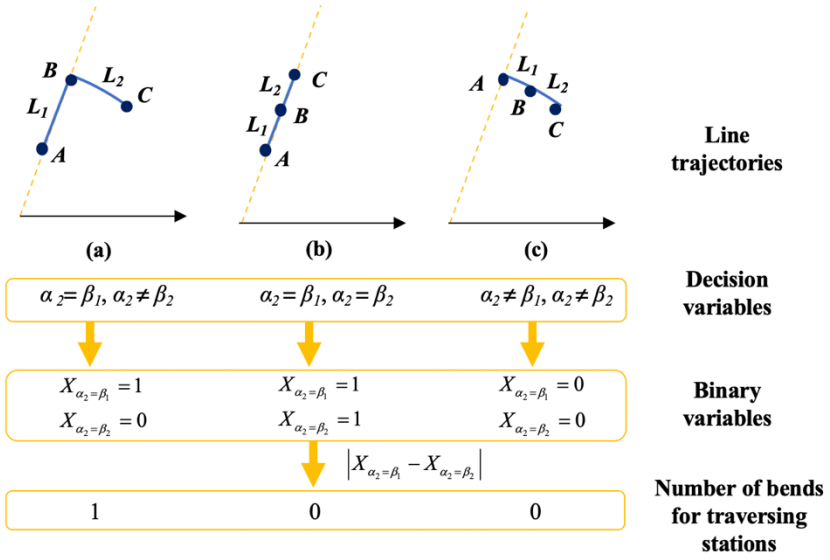

Fig. 7. Possible line trajectories traversing stations

3.4 The MIP model

The modeling procedure is summarized in **Fig. 8**. The map efficiency criteria are modeled as the objectives and constraints of the MIP model. Simplicity and topographicity are modeled as the objectives of the MIP model, and the balanced link length is achieved in the constraints.

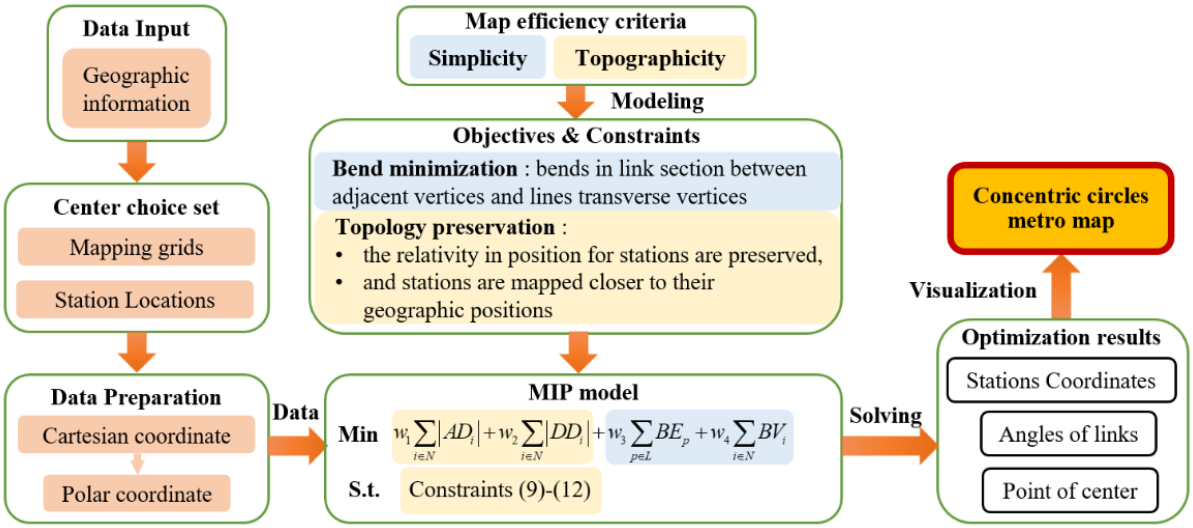

Fig. 8. Summary for the modeling procedure

The MIP model aims at minimizing the distortion of the stations on the generated map, and the bends for the lines. The link length is constrained to be less than the maximum value. The absolute sign can be removed by adding the following constraints:

$$AD_i \geq \alpha_i - \alpha_i^o, i \in N \quad (19)$$

$$AD_i \geq -\alpha_i + \alpha_i^o, i \in N \quad (20)$$

$$DD_i \geq r_i - r_i^o, i \in N \quad (21)$$

$$DD_i \geq -r_i + r_i^o, i \in N \quad (22)$$

$$BV_i \geq X_{\alpha_i=\beta_p} - X_{\alpha_i=\beta_q}, i \in N \quad (23)$$

$$BV_i \geq -X_{\alpha_i=\beta_p} + X_{\alpha_i=\beta_q}, i \in N \quad (24)$$

Overall, the map drawing programming can be formulated by the following MIP model:

$$Min\ w_1\sum_{i\in N}|AD_i| + w_2\sum_{i\in N}|DD_i| + w_3\sum_{p\in L}BE_p + w_4\sum_{i\in N}BV_i \tag{25}$$

s.t. (1) - (12), (19) - (20)

where w_1, w_2, w_3 and w_4 are the weights of different objectives.

4. Numerical experiments

This section provides numerical examples to demonstrate the desirable features of the methodology using a simple network and the applicability using real metro networks of Vienna and Montréal, which have been have been used in (Fink et al., 2014). In this article, we solve the MIP model by Cplex plug-in in Python, and the running time varies from 1-5 seconds depend on the parameters setting. We generated an equivalent expression of Eq. (21) for simpler notations for latter discussion as:

$$Min\ w_1Z_1 + w_2Z_2 + w_3Z_3 + w_4Z_4 \tag{26}$$

where Z_1, Z_2, Z_3 and Z_4 are the notations of different objectives.

4.1 Simple network

A simple network, shown in **Fig. 9**, consists of a loop line with eight stations and eight links to demonstrate the features of proposed methodology. We consider two scenarios of map drawings by weightings adjustment. The purpose of *Scenario 1* is to fully exploit the simplicity of the map drawing by increasing the weights corresponding to total bends (i.e., w_3 and w_4) so that the total number of bends should be zero or close to zero. *Scenario 2* is designed to preserve the original locations of stations by increasing the weights corresponding location distortions (i.e., w_1 and w_2) so that all stations maintain their original locations. The main purpose of this example is to illustrate the modelling process and to demonstrate the discreteness of the two dimensions (simplicity and topographcity) for drawing the metro network in concentric circles. To this end, as shown in **Table 3**, we use the simplest specification for each weighting to amplify the effect of each dimension in the simple network example. The effect of the central point selection and the weight of the optimization objective will be discussed in the real-world examples. There are 24 decision variables that indicate the location of the stations and link sections. 72 binary (intermediate) variables are needed to calculate the bends of the generated concentric circles map. **Fig. 10** summarized the formulations used in the MIP model.

Table 3. Design weight and variables under different scenarios

Scenario	Weights in the objective function				Value of decision variables			
	w_1	w_2	w_3	w_4	Z_1	Z_2	Z_3	Z_4
1	1	1	4	4	0	12.72	0	0
2	4	4	1	1	0	0	8	8

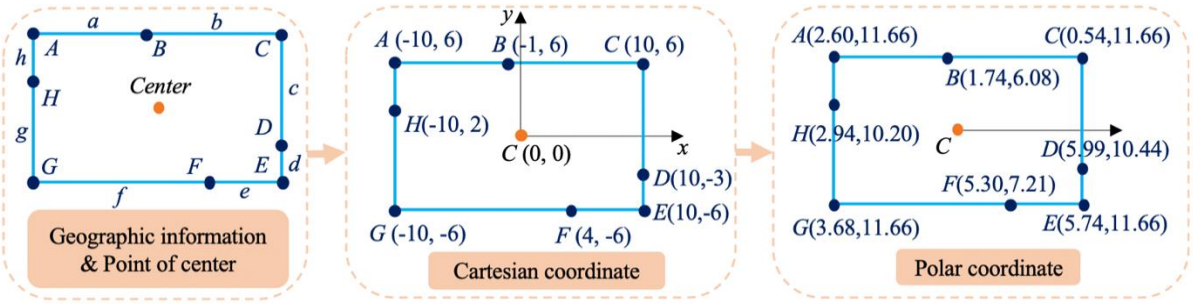

Fig. 9. Simple network

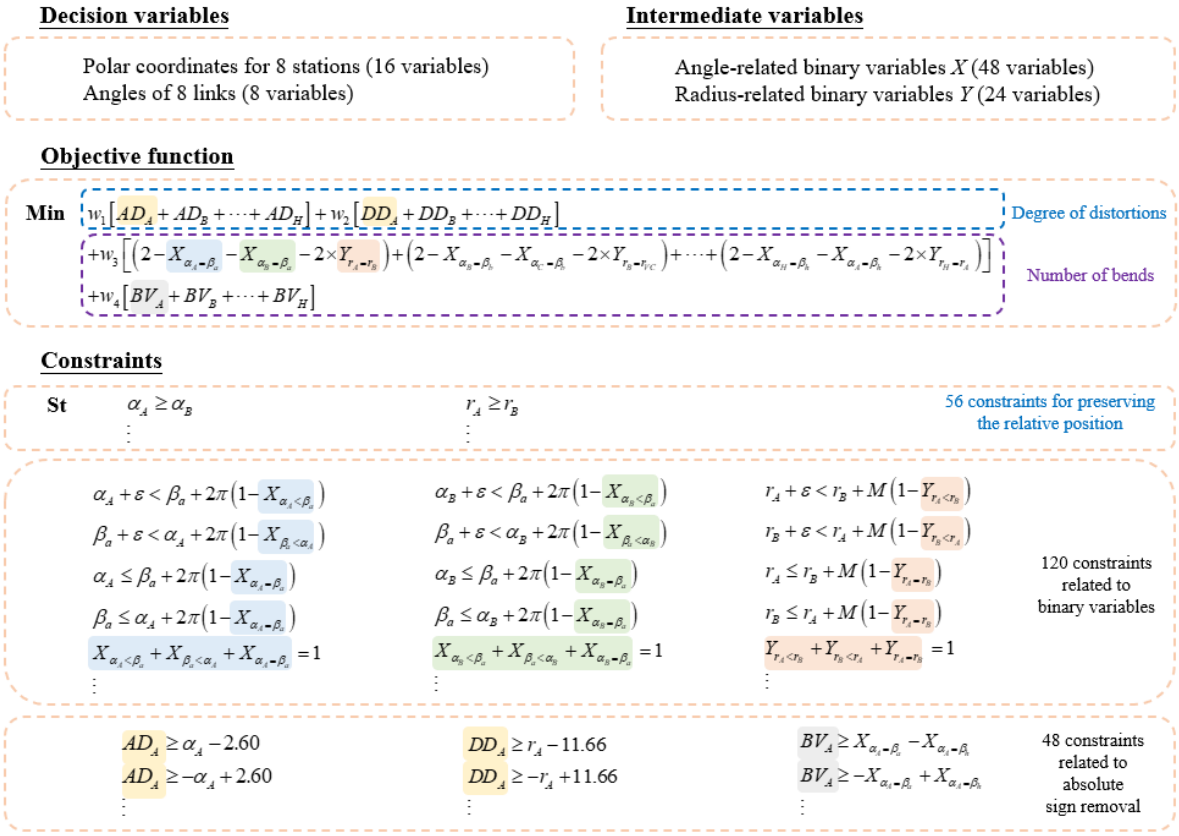

Fig. 10. MIP model for the simple network

4.1.1 Scenario 1: maximizing simplicity

Scenario 1 generates map that most conforms to the simplicity design criteria. The loop line ideally forms a circle in the concentric circle map as shown in **Fig. 11**. All stations have the same radius. Subsequently, they are relocated in the same radial line so that the angle of each station remains unchanged, maintaining zero angular distortion (i.e., $Z_1 = 0$). In this sense, there is no bends for edges and traversing stations (i.e., Z_3, $Z_4 = 0$). While three of four decision variables have been fully optimized (i.e., Z_1, Z_3, $Z_4 = 0$), the linear distortion is sacrificed, where $Z_2 = 12.72$. In this case, the constraints for preserving the relative radius (Eqs. (11)-(12)) of stations are activated, and all the stations keep the angle of the original location.

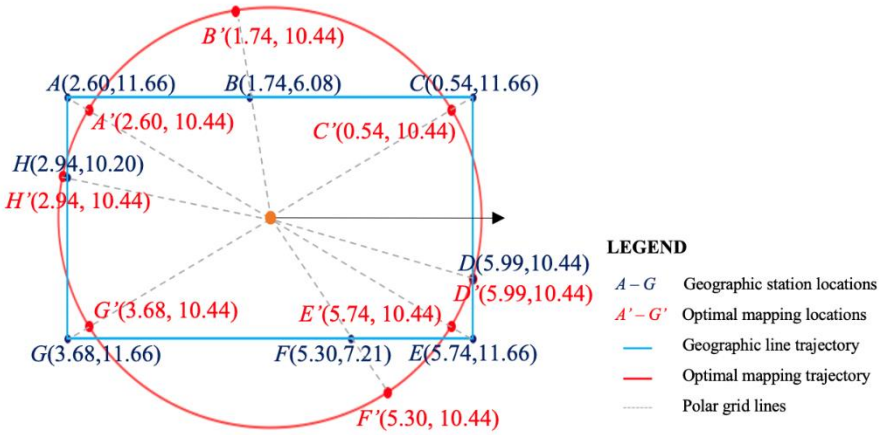

Fig. 11. Mapping results under the scenarios of optimizing simplicity

4.1.2 Scenario 2: maximizing topographcity

Scenario 2 generates map that strictly obey the topographcity criteria. To this end, stations are fixed to their original locations so that there is no location distortion (both angular and linear, i.e., Z_1, $Z_2 = 0$). As shown in **Fig. 12**, since there is no station lie on the same radial or ring line, all the links compose of one ring line and one radial line drawing from a station to the corresponding angle and radius of the adjacent station. This scarifies the simplicity and causes one bend per each station and edge, a total of 16 bends for 8 stations and 8 edges (i.e., Z_3, $Z_4 = 8$).

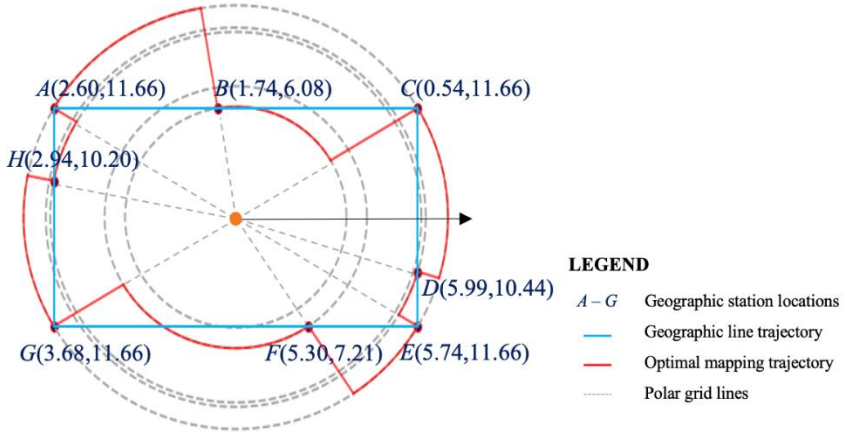

Fig. 12. Mapping results under the scenarios of optimizing topographicity

4.2 Real-world metro networks

We use Vienna and Montréal metro networks to demonstrate the applicability using realistic metro networks of Vienna and Montréal, which have been have been used in Fink et al. (2014). Similar to the representation used by Fink et al. (2014), the line trajectories is input as a simplified network that consists of only transfer and terminal stations. This simplification can facilitate the calculation and map presentation.

4.2.1 Montréal metro network

Montréal metro in Greater Montréal, Quebec, Canada has 4 lines with 68 stations. The simplified network consists of 15 nodes and 16 links that produce 46 variables, 144 binary variables, and 566 constraints. In this section, we examined the effect of the central point

selection with center *A* and *B* which are both the centroid of area surrounded by a loop line as shown in **Fig. 13**. Point *A* is located in a relatively small area surrounded by the green line and orange line, while point *B* is located in the center of a circular line formed by the blue line and orange line.

Table 4. Design weight and variables under different scenarios

Scenario	Weights in the objective function				Value of decision variables			
	w_1	w_2	w_3	w_4	Z_1	Z_2	Z_3	Z_4
A	1	1	1	1	2.38	13.66	7	0
B	1	1	1	1	3.20	9.33	6	3

Offical display maps	Simplified networks
	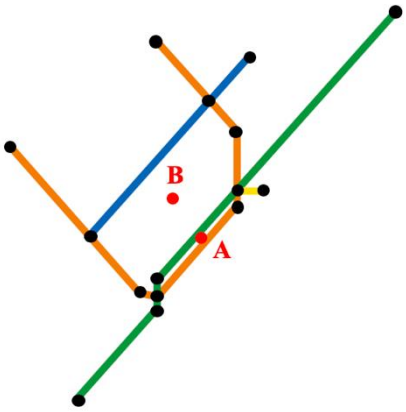

Network information			**Model information**		
4 lines	15 nodes	16 links	46 real variables	144 binary variables	356 constraints

Fig. 13. Vienna and Montréal metro networks

We set w_1, w_2, w_3 and w_4 be 1 for both cases with different point of center (**Table 4**). In **Fig. 14**, for *scenario A*, the visualization shows the congested area with a complete circular line trajectory is enlarged. For *scenario B*, we get a lager circle with the same optimization weight setting. It is hard to determine which is the optimal solution with only the qualitative visualization. When we look at the decision variables, for topographicity Z_1 and Z_2 (i.e., decision variables for angular distortion and distance distortion respectively), *scenario A* preserves more the angular property (i.e., lower value of Z_1) while *scenario B* preserves more the radial property (i.e., lower value of Z_2). In the view of topographicity, the decision on an optimal solution depends on whether which distortion value more subjectively. For simplicity, *scenario A* gives a solution with 7 bends for traversing stations and no bends for edges. In *scenario B*, there are totally 9 bends with 6 bends for traversing stations and 3 bends for edges. For simplicity, *scenario A* generally gives a simpler solution. Overall, with both qualitative and quantitative evaluations, we prefer choosing *A* be the center, considering that a simpler solution with spaces between the green line and orange line enlarged might increase the readability of the concentric circles map.

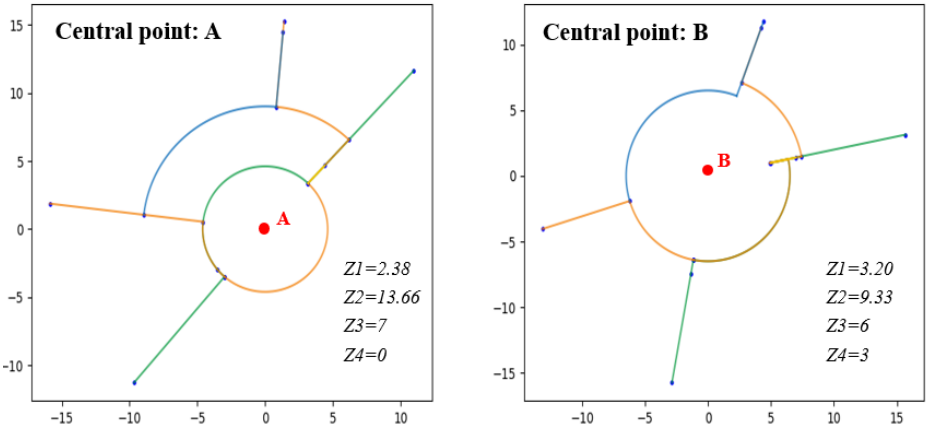

Fig. 14. Automated generated concentric circle map

4.2.2 Vienna metro network

The Vienna U-Bahn is the metro system in Vienna, Austria with 5 lines and 98 stations. We simplified the network with 19 nodes, and 25 links as shown in **Fig. 15**. In this section, we analyzed the effect of adjustable weight parameters *w*. We changed w_1 and w_2, the weights corresponding location distortions, from 0.01 to 20 while maintaining w_3 and w_4 to 1, the weights corresponding to total bends (**Table 5**). The weight of the optimization objective determines the location distortion and number of bends for the generate concentric circles map where can be adjusted to balance the simplicity and topographicity of the map.

Offical display maps	Simplified networks
	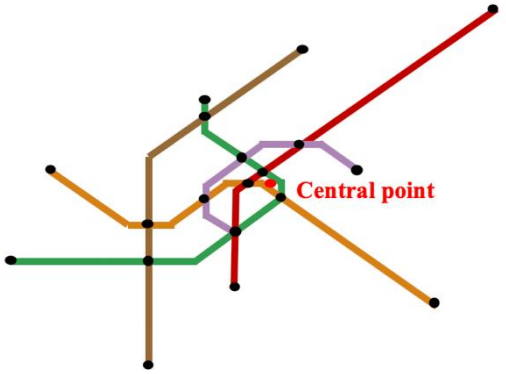

Network information			**Model information**		
5 lines	19 nodes	25 links	63 real variables	225 binary variables	541 constraints

Fig. 15. Montréal metro networks

Table. 5. Design weight and variable under different scenarios

Scenario	Weights in the objective function				Value of decision variables			
	w_1	w_2	w_3	w_4	Z_1	Z_2	Z_3	Z_4
A	0.01	0.01	1	1	0.001	51.92	0	0
B	1	1	1	1	2.72	6.37	11	4
C	5	5	1	1	0.45	0.36	15	19
D	17	17	1	1	0	0	16	25

The corresponding *Z*-value for a range of ratio of weights *RW* are shown in **Fig. 16**. Z_1 and Z_2 (i.e., decision variables for angular distortion and distance distortion respectively) shows their negative correlations in small value of *RW* (i.e., minimizing bends/ maximizing simplicity). It is understandable because under the constraints of position relativity with Eq. (9)-(12), stations are required to preserve its angle of origin location and changes is only allowed in terms of radial distance. This observation further confirms the results we obtained from the case study of the Montréal metro network. Thus, for *scenario A* as shown in **Fig. 16** which aims to minimize bends with very small value of ratio of weights, we can see a circle which is the same result with *scenario 1* of the simple network that minimizes bends as shown in **Fig. 11**, with all constraints for the relative distance (i.e., Eqs.(11)-(12)) are activated. In this case, almost all nodes located on the same ring line that cause the largest radius distortion (i.e., Z_2 = 51.92). *Scenario B* shows a balanced optimal solution with all *Z*-value equal to one. When we move along the x-axis in **Fig. 16**, the value of Z_1 and Z_2 tend to zero, which indicates a nearly optimal solution in terms of simplicity can be obtained at *RW* value of 5. Thus, for *scenario C*, we can see Z_1 and Z_2 is close to zero, and Z_3 and Z_4 (i.e., decision variables for bends of edges and traversing stations respectively) is high, with 15 bends for traversing nodes and 19 bends for edges. The highest value of Z_3 and Z_4 can be obtain at the *RW* value of 15.4, with Z_1 and Z_2 equal to zero, resulted in *scenario D*. There are 16 bends for traversing nodes, and 25 bends for edges, with original locations are totally preserved. In conclude, the above results show the effects of weights in determining the local optimal solutions, while the global one depends on the user preference about different parameters.

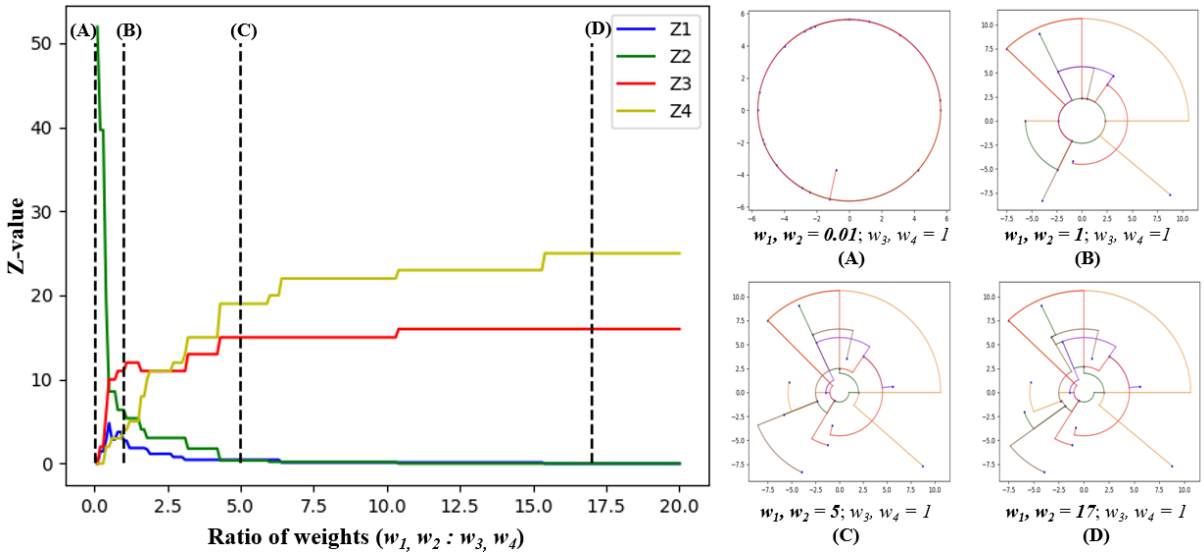

Fig. 16. Automated generated concentric circle map

5. Conclusions

In this article, we present an automatic concentric circles map drawing method by integrating the map usability design criteria into the mixed-integer programming (MIP). We demonstrate the validity of the proposed model with several numerical experiments with a simple network and two real-world metro networks. Our proposed algorithm allows us to generate prototypes of concentric circle metro maps quickly with some flexibility in the weight parameter settings. We showed that the choice of center and the weights between decision variables about distortion and bends could affect the optimal solution obtained. This subsequently allows to highlight the importance of quantified measurements to evaluate the quality of solutions in both qualitative

and quantitative way. The experiments presented show that our method is feasible for visualizing both medium and medium-large real metro networks. We showed that the proposed technique for components is capable of covering the variance of users' needs.

As future work, we want to investigate the optimal choices of center, by integrating it into the objective function. In the current stage, the choice of center is determined subjectively by users. We therein plan to put the emphasis of future research on the optimal choices of center. Further, we will work on improving the coherence of the visualization (e.g., metro lines being overlapped). We also want to investigate the feasibility for an interactive approach, which is started to be explored in the octo-linear metro maps (van Dijk and Haunert, 2014; Wang and Peng, 2016; Wilson et al., 2010).

1

References

Barth, L., 2016. Drawing metro maps on concentric circles. M.S. thesis, Department of Informatics, Karlsruhe Institute of Technology, Karlsruhe, Germany.

Bertault, F., 2000. A force-directed algorithm that preserves edge-crossing properties 74, 7–13.

Chan, H.-Y., Chen, A., Li, G., Xu, X., Lam, W., 2021. Evaluating the value of new metro lines using route diversity measures: The case of Hong Kong's Mass Transit Railway system. J. Transp. Geogr. 91, 102945. https://doi.org/10.1016/j.jtrangeo.2020.102945

Chan, R., 2018. My iterations of the MTR system map [WWW Document]. URL https://roychan.home.blog/mtr/ (accessed 3.9.21).

Fink, M., Haverkort, H., Martin, N., Roberts, M., 2012. Drawing metro maps using B´ezier curves, in: Proceedings of the 20th International Conference on Graph Drawing. pp. 463–474.

Fink, M., Lechner, M., Wolff, A., 2014. Concentric metro maps, in: Schematic Mapping Workshop 2014, University of Essex, April. pp. 1–2.

Frick, A., Ludwig, A., Mehldau, H., 1995. A fast adaptive layout algorithm for undirected graphs. Graph Draw. 94, Lect. Notes Comput. Sci. 894.

Hong, S., Merrick, D., do Nascimento, H.A.D., 2006. Automatic visualisation of metro maps. J. Vis. Lang. Comput. 17, 203–224. https://doi.org/10.1016/j.jvlc.2005.09.001

Konovalov, C., 2016. The new Paris metro map [WWW Document]. metromap. URL http://metromap.fr/en (accessed 3.9.21).

Kozo Sugiyama; Kazuo Misue, 1995. Graph drawing by the magnetic spring model. J. Vis. Lang. Comput. 6, 217–231.

Lan, T., Li, Z., Ti, P., 2019. Integrating general principles into mixed-integer programming to optimize schematic network maps. Int. J. Geogr. Inf. Sci. 33, 2305–2333. https://doi.org/10.1080/13658816.2019.1620237

Li, Z., 2015. General principles for automated generation of schematic network maps. Cartogr. J. 52, 356–360. https://doi.org/10.1080/00087041.2015.1108661

Li, Z., Dong, W., 2010. A stroke-based method for automated generation of schematic network maps 8816. https://doi.org/10.1080/13658811003766936

Nöllenburg, M., Wolff, A., 2011. Drawing and labeling high-quality metro maps by mixed-integer programming. IEEE Trans. Vis. Comput. Graph. 17, 626–641. https://doi.org/10.1109/TVCG.2010.81

Ovenden, M., 2015. Metro maps of the world, 2nd ed, Penguin Books. New York.

Roberts, M.J., 2019. Us versus them: Ensuring practical and psychological utility of measurements of schematic map usability, in: Schematic Mapping Workshop 2019. TU Wien, April., pp. 1–6.

Roberts, M.J., 2014. What's your theory of effective schematic map design? First Int. Schematic Mapp. Work.

Roberts, M.J., 2013. The story of circles maps [WWW Document]. Tube Map Cent. URL http://www.tubemapcentral.com/writing/webarticles/circles/circles.html

Roberts, M.J., Newton, E.J., Canals, M., 2016. Radi(c)al departures: comparing conventional octolinear versus concentric circles schematic maps for the Berlin U-Bahn/S-Bahn networks using objective and subjective measures of effectiveness. Inf. Des. J. 22, 92–115. https://doi.org/10.1075/idj.22.2.04rob

Roberts, M.J., Newton, E.J., Lagattolla, F.D., Hughes, S., Hasler, M.C., 2013. Objective versus subjective measures of Paris metro map usability: Investigating traditional octolinear versus all-curves schematics. J. Hum. Comput. Stud. 71, 363–386.

https://doi.org/10.1016/j.ijhcs.2012.09.004
Saidi, S., Ji, Y., Cheng, C., Guan, J., Jiang, S., Kattan, L., Du, Y., Wirasinghe, S.C., 2016a. Planning urban ring rail transit lines: Case study of Shanghai, China. Transp. Res. Rec. 2540, 56–65. https://doi.org/10.3141/2540-07
Saidi, S., Wirasinghe, S.C., Kattan, L., 2016b. Long-term planning for ring-radial urban rail transit networks. Transp. Res. Part B Methodol. 86, 128–146. https://doi.org/https://doi.org/10.1016/j.trb.2016.01.017
Saidi, S., Wirasinghe, S.C., Kattan, L., Esmaeilnejad, S., 2017. A generalized framework for complex urban rail transit network analysis. Transp. A Transp. Sci. 13, 874–892. https://doi.org/10.1080/23249935.2017.1348401
Sester, M., 2005. Optimization approaches for generalization and data abstraction. Int. J. Geogr. Inf. Sci. 19, 871–897. https://doi.org/10.1080/13658810500161179
Stott, J., Rodgers, P., Martinnez-Ovando, J.C., Walker, S.G., 2011. Automatic metro map layout using multicriteria optimization. IEEE Trans. Vis. Comput. Graph. 17, 101–114. https://doi.org/10.1109/TVCG.2010.24
Szabo, P., Genge, B., 2019. Circle map for Internet of Things networks. 7th Int. Symp. Digit. Forensics Secur. ISDFS 2019. https://doi.org/10.1109/ISDFS.2019.8757541
Ti, P., Li, Z., 2014. Generation of schematic network maps with automated detection and enlargement of congested areas. Int. J. Geogr. Inf. Sci. 28, 521–540. https://doi.org/10.1080/13658816.2013.855313
Tseng, T., 2017. Taipei metro map in concentric circle style [WWW Document]. URL https://www.behance.net/gallery/76488827/-Taipei-Metro-Map-in-Concentric-Circle-Style
van Dijk, T.C., Haunert, J.H., 2014. Interactive focus maps using least-squares optimization. Int. J. Geogr. Inf. Sci. 28, 2052–2075. https://doi.org/10.1080/13658816.2014.887718
Wang, Y.S., Chi, M.T., 2011. Focus plus context metro maps. IEEE Trans. Vis. Comput. Graph. 17, 2528–2535.
Wang, Y.S., Peng, W.Y., 2016. Interactive metro map editing. IEEE Trans. Vis. Comput. Graph. 22, 1115–1126. https://doi.org/10.1109/TVCG.2015.2430290
Wilson, D., Bertolotto, M., Weakliam, J., 2010. Personalizing map content to improve task completion efficiency. Int. J. Geogr. Inf. Sci. 24, 741–760. https://doi.org/10.1080/13658810903074490
Wolmar, C., 2009. The Subterranean railway: How the London Underground was built and how it changed the city forever, 48010th ed. ed. Atlantic Books Ltd.
Wu, H., Niedermann, B., Takahashi, S., Roberts, M.J., Nöllenburg, M., 2020. A survey on transit map layout: from design, machine, and human perspectives, in: Computer Graphics Forum (Proceedings of EuroVis 2020). pp. 1–28.